Dynamical Generation of Hyperon Resonances

A. Ramos,[a] E. Oset,[b] **C.** Bennhold, [c] D. Jido,[d]
J.A. Oller [e] and U.-G. Meißner[f] [g]

[a]Departament d'Estructura i Constituents de la Matèria, Universitat de Barcelona,
Diagonal 647, 08028 Barcelona, Spain

[b]Departamento de Física Teórica and IFIC, Centro Mixto Universidad de
Valencia-CSIC,
Institutos de Investigación de Paterna, Aptd. 22085, 46071 Valencia, Spain

[c]Center for Nuclear Studies, Department of Physics,
The George Washington University, Washington D.C. 20052 , USA

[d]ECT*, Villa Tambosi, Strada delle Tabarelle 286, I-38050 Villazano (Trento), Italy

[e]Departamento de Física, Universidad de Murcia, 30071 Murcia, Spain

[f]Universität Bonn, Helmholtz-Institut für Strahlen- und Kernphysik (Theorie)
Nußalle 14-16, D-53115 Bonn, Germany

[g] FZ Jülich, IKP (TH), D-52425 Jülich, Germany

In this talk we report on how, using a chiral unitary approach for the meson–baryon in-
teractions, two octets of $J^\pi = 1/2^-$ baryon states and a singlet are generated dynamically,
resulting in the case of strangeness $S = -1$ in two poles of the scattering matrix close to
the nominal $\Lambda(1405)$ resonance. We suggest experiments which could show evidence for
the existence of these states.

1. Introduction

The introduction of unitarity constraints in coupled channels in chiral perturbation
theory has led to unitary extensions of the theory that starting from the same effective
Lagrangians allow one to make predictions at much higher energies. One of the interesting
consequences of these extensions is that they generate dynamically low lying resonances,
both in the mesonic and baryonic sectors. By this we mean that they are generated by the
multiple scattering of the meson or baryon components, much the same as the deuteron
is generated by the interaction of the nucleons through the action of a potential, and they
are not preexistent states that remain in the large N_c limit where the multiple scattering
is suppressed. In what follows we show how two octets and a singlet of such states are
generated in the baryon sector with $J^P = 1/2^-$, with properties in good agreement with
existing resonances. In the strangeness $S = -1$ case the lowest lying of such resonances

is the $\Lambda(1405)$. The $\Lambda(1405)$ resonance is a clear example of a dynamically generated resonance appearing naturally in scattering theory with coupled meson–baryon channels with strangeness $S = -1$ [1]. Chiral formulations of the meson–baryon interaction within unitary frameworks all lead to the generation of this resonance, which is seen in the mass distribution of $\pi\Sigma$ states with isospin $I = 0$ in hadronic production processes [2, 3, 4, 5]. Yet, it was shown that in some models one could obtain two poles close to the nominal $\Lambda(1405)$ resonance, as it was the case within the cloudy bag model in Ref. [6]. Also, in the investigation of the poles of the scattering matrix in Ref. [4], within the context of chiral dynamics, it was found that there were two poles close to the nominal $\Lambda(1405)$ resonance both contributing to the $\pi\Sigma$ invariant mass distribution. This was also the case in Refs. [7, 8], where two poles are obtained with similar properties as to their masses, widths and partial decay widths compared to those of the previous works.

The discussion below will clarify this issue and the structure of these resonances.

2. Description of the meson baryon interactions

Starting from the chiral Lagrangians for meson–baryon interactions [9] and using the N/D method to obtain a scattering matrix fulfilling exactly unitarity in coupled channels [4], the full set of transition matrix elements with the coupled channels in $S = -1$, K^-p, $\bar{K}^0n$, $\pi^0\Lambda$, $\pi^0\Sigma^0$, $\pi^+\Sigma^-$, $\pi^-\Sigma^+$, $\eta\Lambda$, $\eta\Sigma^0$, $K^0\Xi^0$ and $K^+\Xi^-$, is given in matrix form by

$$T = [1 - V\,G]^{-1}\,V \ . \tag{1}$$

Here, the matrix V, obtained from the lowest order meson–baryon chiral Lagrangian, contains the Weinberg-Tomozawa or seagull contribution, as employed e.g. in Ref. [10],

$$V_{ij} = -C_{ij}\frac{1}{4f^2}(2\sqrt{s} - M_i - M_j)\left(\frac{M_i + E}{2M_i}\right)^{1/2}\left(\frac{M_j + E'}{2M_j}\right)^{1/2} \ , \tag{2}$$

where the C_{ij} coefficients are given in Ref. [3], and an averaged meson decay constant $f = 1.123f_\pi$ is used [10], with $f_\pi = 92.4\,\text{MeV}$ the weak pion decay constant. At lowest order in the chiral expansion all the baryon masses are equal to the one in the chiral limit, M_0, nevertheless in Ref. [10] the physical baryon masses, M_i, were used and these are the ones appearing in Eq. (2). In addition to the Weinberg-Tomozawa term, one also has at the same order in the chiral expansion the direct and exchange diagrams considered in Ref. [4]. These are suppressed at low energies by powers of the three-momenta and meson masses over M_i, the leading one being just linear. However, their importance increases with energy and around $\sqrt{s} \simeq 1.5$ GeV they can be as large as a 20 percent of the seagull term.

The diagonal matrix G stands for the loop function of a meson and a baryon and is defined by a subtracted dispersion relation in terms of phase space with a cut starting at the corresponding threshold [4]. It corresponds to the loop function of a meson and a baryon once the logarithmic divergent constant is removed.

The analytical properties of G are properly kept when evaluating the previous loop function in dimensional regularization. Using dimensional regularization and removing

the divergent constant piece leads to

$$
\begin{aligned}
G_l &= i\,2M_l \int \frac{d^4q}{(2\pi)^4} \frac{1}{(P-q)^2 - M_l^2 + i\epsilon} \frac{1}{q^2 - m_l^2 + i\epsilon} \\
&= \frac{2M_l}{16\pi^2} \left\{ a_l(\mu) + \ln\frac{M_l^2}{\mu^2} + \frac{m_l^2 - M_l^2 + s}{2s} \ln\frac{m_l^2}{M_l^2} + \right. \\
&\quad + \frac{q_l}{\sqrt{s}} \left[\ln(s - (M_l^2 - m_l^2) + 2q_l\sqrt{s}) + \ln(s + (M_l^2 - m_l^2) + 2q_l\sqrt{s}) \right. \\
&\quad \left.\left. - \ln(-s + (M_l^2 - m_l^2) + 2q_l\sqrt{s}) - \ln(-s - (M_l^2 - m_l^2) + 2q_l\sqrt{s}) \right] \right\} ,
\end{aligned} \tag{3}
$$

where μ is the scale of dimensional regularization. For a given value of this scale, the subtraction constant $a_i(\mu)$ is determined so that the results are finally scale independent.

This meson baryon loop function was calculated in Ref. [3] with a cut-off regularization, similarly as previously done in meson–meson scattering [14]. The values of the a_i constants in Eq. (3) are found to be around -2 to agree with the results of the cut–off method for cut–off values of the order of the mass of the $\rho(770)$ [4], which we call of natural size. Indeed, in Ref. [10] it was found that with the values for the subtraction constants

$$
\begin{aligned}
a_{\bar{K}N} &= -1.84 , & a_{\pi\Sigma} &= -2.00 , & a_{\pi\Lambda} &= -1.83 , \\
a_{\eta\Lambda} &= -2.25 , & a_{\eta\Sigma} &= -2.38 , & a_{K\Xi} &= -2.67 ,
\end{aligned} \tag{4}
$$

one reproduces the results for the G functions obtained in Ref. [3] with a cut–off of 630 MeV.

3. Poles of the T-matrix

The study of Ref. [10] showed the presence of poles in Eq. (1) around the $\Lambda(1405)$ and the $\Lambda(1670)$ for isospin $I = 0$ and around the $\Sigma(1620)$ in $I = 1$. The same approach in $S = -2$ leads to the resonance $\Xi(1620)$ [11] and in $S = 0$ to the $N^*(1535)$ [12, 13], this latter one also generated dynamically in Ref. [12]. One is thus tempted to consider the appearance of a singlet and an octet of meson–baryon resonances. Nevertheless, the situation is more complicated because indeed in the SU(3) limit there are *two* octets and not just one, as we discuss below. The presence of these multiplets was already discussed in Ref. [4] after obtaining a pole with $S = -1$ in the $I = 1$ channel, with mass around 1430 MeV, and two poles with $I = 0$, of masses around that of the $\Lambda(1405)$. Similar ideas have been exploited in the meson–meson interaction where a nonet of dynamically generated mesons, made of the $\sigma(500)$, $f_0(980)$, $a_0(980)$ and $\kappa(900)$, has been obtained [14, 15, 16, 17].

The appearance of a multiplet of dynamically generated mesons and baryons seems most natural once a state of the multiplet appears. Indeed, one must recall that the chiral Lagrangians are obtained from the combination of the octet of pseudoscalar mesons (the pions and partners) and the octet of stable baryons (the nucleons and partners). The SU(3) decomposition of the combination of two octets tells us that

$$
8 \otimes 8 = 1 \oplus 8_s \oplus 8_a \oplus 10 \oplus \overline{10} \oplus 27 . \tag{5}
$$

Thus, on pure SU(3) grounds, should we have a SU(3) symmetric Lagrangian, one can expect e.g. one singlet and two octets of resonances, the symmetric and antisymmetric ones. Actually in the case of the meson–meson interactions only the symmetric octet appears in S-wave because of Bose statistics, but in the case of the meson–baryon interactions, where the building blocks come from two octets of different nature, both the symmetric and antisymmetric octets could appear and there is no reason why they should be degenerate in principle.

The lowest order meson–baryon chiral Lagrangian is exactly SU(3) invariant if all the masses of the mesons are set equal. As stated above [see Eq. (2)], in Ref. [10] the baryon masses take their physical values, although strictly speaking at the leading order in the chiral expansion they should be equal to M_0. For Eq. (2) being SU(3) symmetric, all the baryons masses M_i must be set equal as well. When all the meson and baryon masses are equal, and these common masses are employed in evaluating the G_l functions, together with equal subtraction constants a_l, the T–matrix obtained from Eq. (1) is also SU(3) symmetric.

If we do such an SU(3) symmetry approximation and look for poles of the scattering matrix, we find poles corresponding to the octets and singlet. The surprising result is that the two octet poles are degenerate as a consequence of the dynamics contained in the chiral Lagrangians. Indeed, if we evaluate the matrix elements of the transition potential V in a basis of SU(3) states,

$$V_{\alpha\beta} = \sum_{i,j} \langle i, \alpha \rangle C_{ij} \langle j, \beta \rangle, \tag{6}$$

where $\langle i, \alpha \rangle$ are the SU(3) Clebsch–Gordan coefficients and C_{ij} the coefficients in Eq. (2), we obtain:

$$V_{\alpha\beta} = \mathrm{diag}(6, 3, 3, 0, 0, -2) , \tag{7}$$

taking the following order for the irreducible representations: 1, 8_s, 8_a, 10, $\overline{10}$ and 27.

Hence we observe that the states belonging to different irreducible representations do not mix and the two octets appear degenerate. The coefficients in Eq. (7) clearly illustrate why there are no bound states in the 10, $\overline{10}$ and 27 representations. Indeed, considering the minus sign in Eq. (2), a negative sign in Eq. (7) means repulsion.

In practice, the same chiral Lagrangians allow for SU(3) breaking. In the case of Refs. [3, 10] the breaking appears because both in the V_{ij} transition potentials as in the G_l loop functions one uses the physical masses of the particles as well as different subtraction constants in G_l, corresponding to the use of a unique cut-off in all channels. In Ref. [4] the physical masses are also used in the G_l functions, although these functions are evaluated with a unique subtraction constant as corresponds to the SU(3) limit. In addition, the V_{ij} transition potentials are evaluated strictly at lowest order in the chiral expansion, so that a common baryon mass is used and the one baryon exchange diagrams, both direct and crossed, are included. In both approaches, physical masses are used to evaluate the G_l loop functions so that unitarity is fulfilled exactly and the physical thresholds for all channels are respected.

By following the approach of Ref. [10] and using the physical masses of the baryons and the mesons, the position of the poles change and the two octets split apart in four
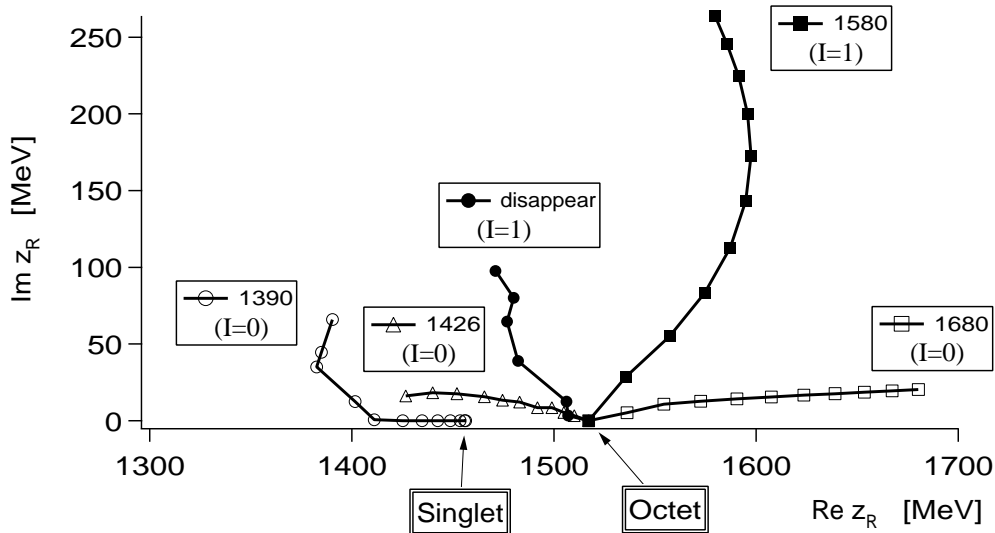
Figure 1. Trajectories of the poles in the scattering amplitudes obtained by changing the SU(3) breaking parameter x gradually. At the SU(3) symmetric limit ($x = 0$), only two poles positions appear, one for the singlet and the other for the octet. The symbols correspond to the step size $\delta x = 0.1$. The results are from [18].

branches, two for $I = 0$ and two for $I = 1$, as one can see in Fig. 1. In the figure we show the trajectories of the poles as a function of a parameter x that breaks gradually the SU(3) symmetry up to the physical values. The dependence of masses and subtraction constants on the parameter x is given by

$$M_i(x) = M_0 + x(M_i - M_0), \quad m_i^2(x) = m_0^2 + x(m_i^2 - m_0^2), \quad a_i(x) = a_0 + x(a_i - a_0), \quad (8)$$

where $0 \leq x \leq 1$. For the baryon masses, $M_i(x)$, the breaking of the SU(3) symmetry follows linearly, while for the meson masses, $m_i(x)$, the law is quadratic in the masses, since in the QCD Lagrangian the flavor SU(3) breaking appears in the quark mass terms and the squares of the meson masses depend on the quark masses linearly. In the calculation of Fig. 1, the values $M_0 = 1151$ MeV, $m_0 = 368$ MeV and $a_0 = -2.148$ are used.

The complex poles, z_R, appear in unphysical sheets. In the present search we follow the strategy of changing the sign of the momentum q_l in the $G_l(z)$ loop function of Eq. (3) for the channels which are open at an energy equal to Re(z).

The splitting of the two $I = 0$ octet states is very interesting. One moves to higher energies giving rise to the $\Lambda(1670)$ resonance and the other one moves to lower energies to create a pole, quite well identified below the $\bar{K}N$ threshold, with a narrow width. We should also note that when for some values of x the trajectory crosses the $\bar{K}N$ threshold (~ 1435 MeV) the pole fades away but it emerges again clearly for values of x close to 1. On the other hand, the singlet also evolves to produce a pole at low energies with a quite large width.

We note that the singlet and the $I = 0$ octet states appear nearby in energy and one

of the purposes of this paper is, precisely, to point out the fact that what experiments actually see is a combination of the effect of these two resonances.

Similarly as for the $I = 0$ octet states, we can see that one branch of the $I = 1$ states moves to higher energies while another moves to lower energies. The branch moving to higher energies finishes at what would correspond to the $\Sigma(1620)$ resonance when the physical masses are reached. The branch moving to lower energies fades away after a while when getting close to the $\bar{K}N$ threshold.

The model of Ref. [4] reproduces qualitatively the same results. However, this model also produces in the physical limit ($x = 1$) another $I = 1$ pole having $\mathrm{Re}(z)$=1401 MeV if, in addition to changing the signs of the on-shell momenta in the $\pi\Lambda$ and $\pi\Sigma$ channels in accordance to the strategy mentioned above, the sign in the $\bar{K}N$ channel is also changed. The fact is that in both approaches there is a $I = 1$ amplitude with an enhanced strength around the $\bar{K}N$ thhrehold. Whether this enhancement in the $I = 1$ amplitude can be interpreted as a resonance or as a cusp, the fact that the strength of the $I = 1$ amplitude around the $\Lambda(1405)$ region is not negligible should have consequences for reactions producing $\pi\Sigma$ pairs in that region. This has been illustrated for instance in Ref. [19], where the photoproduction of the $\Lambda(1405)$ via the reaction $\gamma p \rightarrow K^{+}\Lambda(1405)$ was studied. It was shown there that the different sign in the $I = 1$ component of the $\mid \pi^{+}\Sigma^{-}\rangle$, $\mid \pi^{-}\Sigma^{+}\rangle$ states leads, through interference between the $I = 1$ and the dominant $I = 0$ amplitudes, to different cross sections in the various charge channels, a fact that has been confirmed experimentally very recently [20].

Once the pole positions are found, one can also determine the couplings of these resonances to the physical states by studying the amplitudes close to the pole and identifying them with

$$T_{ij} = \frac{g_i g_j}{z - z_R} \ . \tag{9}$$

The couplings g_i are in general complex valued numbers. In Table 1 we summarize the pole positions and the complex couplings g_i obtained from the model of Ref. [10] for isospin $I = 0$. The results with the model of [4] are qualitatively similar.

Table 1
Pole positions and couplings to $I = 0$ physical states from the model of Ref. [10]

z_R	$1390 + 66i$		$1426 + 16i$		$1680 + 20i$	
($I = 0$)	g_i	$\lvert g_i \rvert$	g_i	$\lvert g_i \rvert$	g_i	$\lvert g_i \rvert$
$\pi\Sigma$	$-2.5 - 1.5i$	2.9	$0.42 - 1.4i$	1.5	$-0.003 - 0.27i$	0.27
$\bar{K}N$	$1.2 + 1.7i$	2.1	$-2.5 + 0.94i$	2.7	$0.30 + 0.71i$	0.77
$\eta\Lambda$	$0.010 + 0.77i$	0.77	$-1.4 + 0.21i$	1.4	$-1.1 - 0.12i$	1.1
$K\Xi$	$-0.45 - 0.41i$	0.61	$0.11 - 0.33i$	0.35	$3.4 + 0.14i$	3.5

We now consider the results obtained from the model of Ref. [4]. Making use of their set I of parameters, which correspond to a baryon mass $M_0 = 1286$ MeV and a meson

Table 2

Pole positions and couplings to $I = 1$ physical states from the model of Ref. [4]

z_R $(I = 1)$	$1401 + 40i$		$1488 + 114i$	
	g_i	$|g_i|$	g_i	$|g_i|$
$\pi\Lambda$	$0.60 + 0.47i$	0.76	$0.98 + 0.84i$	1.3
$\pi\Sigma$	$1.27 + 0.71i$	1.5	$-1.32 - 1.00i$	1.7
$\bar{K}N$	$-1.24 - 0.73i$	1.4	$-0.89 - 0.57i$	1.1
$\eta\Sigma$	$0.56 + 0.41i$	0.69	$0.58 + 0.29i$	0.65
$K\Xi$	$0.12 + 0.05i$	0.13	$-1.63 - 0.91i$	1.9

decay constant $f = 0.798 f_\pi = 74.1$ MeV, both in the chiral limit, together with a common subtraction constant $a = -2.23$, the results obtained for $I = 1$ are displayed in Table 2.

We observe that the second resonance with $I = 0$ couples strongly to $\bar{K}N$ channel, while the first resonance couples more strongly to $\pi\Sigma$. The results for $I = 0$ shown in Table 1 resemble much those obtained in Ref. [6] and Ref. [8] where two resonances are also found close to 1405 MeV, with the one at lower energies having a larger width than the second and a stronger coupling to $\pi\Sigma$, while the resonance at higher energies being narrower and coupling mostly to $\bar{K}N$.

We can also project the states found over the pure SU(3) states and we find the results of Table 3

Table 3

Couplings of the $I = 0$ bound states to the meson–baryon SU(3) basis states, obtained with the model of Ref. [10]

z_R	$1390 + 66i$ (evolved singlet)		$1426 + 16i$ (evolved octet 8_s)		$1680 + 20i$ (evolved octet 8_a)	
	g_γ	$|g_\gamma|$	g_γ	$|g_\gamma|$	g_γ	$|g_\gamma|$
1	$2.3 + 2.3i$	3.3	$-2.1 + 1.6i$	2.6	$-1.9 + 0.42i$	2.0
8_s	$-1.4 - 0.14i$	1.4	$-1.1 - 0.62i$	1.3	$-1.5 - 0.066i$	1.5
8_a	$0.53 + 0.94i$	1.1	$-1.7 + 0.43i$	1.8	$2.6 + 0.59i$	2.7
27	$0.25 - 0.031i$	0.25	$0.18 + 0.092i$	0.21	$-0.36 + 0.28i$	0.4

We observe that the physical singlet couples mostly to the singlet SU(3) state. This means that this physical state has retained largely the singlet nature it had in the SU(3) symmetric situation. The same is true for the physical $I = 0$ antisymmetric octet shown in the last column. However, the couplings of the physical symmetric octet reveal that, due to its proximity to the singlet state, it has become mostly a singlet with some admixture of the symmetric and antisymmetric octets.

4. Influence of the poles on the physical observables

In a given reaction the $\Lambda(1405)$ resonance is always seen in $\pi\Sigma$ mass distribution. However, this final state can be reached through the production of any intermediate state which couples to the $\pi\Sigma$ state, since the final state interaction will reshufle the channels as we have seen in the chiral unitary approach. Hence, the mass distribution of $\pi\Sigma$ will be given by

$$\frac{d\sigma}{dM_i} = |\sum_i C_i T_{i\to\pi\Sigma}|^2 q_{\text{c.m.}} \; , \tag{10}$$

where the C_i coefficients depend on the dynamics of the particular problem. This is curious since practically in all approaches where the $\Lambda(1405)$ is claimed to be obtained one uses the equation

$$\frac{d\sigma}{dM_i} = C|T_{\pi\Sigma\to\pi\Sigma}|^2 q_{\text{c.m.}} \; , \tag{11}$$

where C is a constant, which has no justification. Indeed, if the sum in eq. (11) were dominated by the $\bar{K}N \to \pi\Sigma$ amplitude, then the second resonance R_2 would be weighted more, since it has a stronger coupling to the $\bar{K}N$ state, resulting into an apparent narrower resonance peaking at higher energies. This can be seen in Fig. 2. In ref. [4] the C_i coefficients foor $\bar{K}N$ and $\pi\Sigma$ were fitted to the data. The fact is that if there were only one resonance eqs. (10) and (11) would lead to the same shape of the distribution since all the amplitudes would have the same resonance shape. But the existence of two poles makes the sum in eq. (10) dependent on the weights C_i and then dependent on the particular reaction. Hence, from now on, a theoretical claim about understanding the $\Lambda(1405)$ properties has to be substanciated by a simultaneous theoretical analysis of the particular reaction where this resonance has been seen. In this sense, there is a recent work [21] in which the dynamics of the $\pi^- p \to K^0 \pi\Sigma$, from where the nominal $\Lambda(1405)$ resonance comes, has been studied and the particular shape of the resonance found in this reaction is traced back to a nontrivial combination of chiral mechanisms involving the meson pole and contact term in the $MB \to MMB$ amplitudes together with the contribution of the s-wave $N^*(1710)$ resonance which has a strong coupling to the MMB system, as proved by the large decay width into $\pi\pi N$.

It is clear that, should there be a reaction which forces the initial channels to be $\bar{K}N$, then this would give more weight to the second resonance, R_2, and hence produce a distribution with a shape corresponding to an effective resonance narrower than the nominal one and at higher energy. Such a case indeed occurs in the reaction $K^- p \to \Lambda(1405)\gamma$ studied theoretically in Ref. [22]. It was shown there that since the $K^- p$ system has a larger energy than the resonance, one has to lose energy emitting a photon prior to the creation of the resonance and this is effectively done by the Bremsstrahlung from the original K^- or the proton. Hence the resonance is initiated from the $K^- p$ channel.
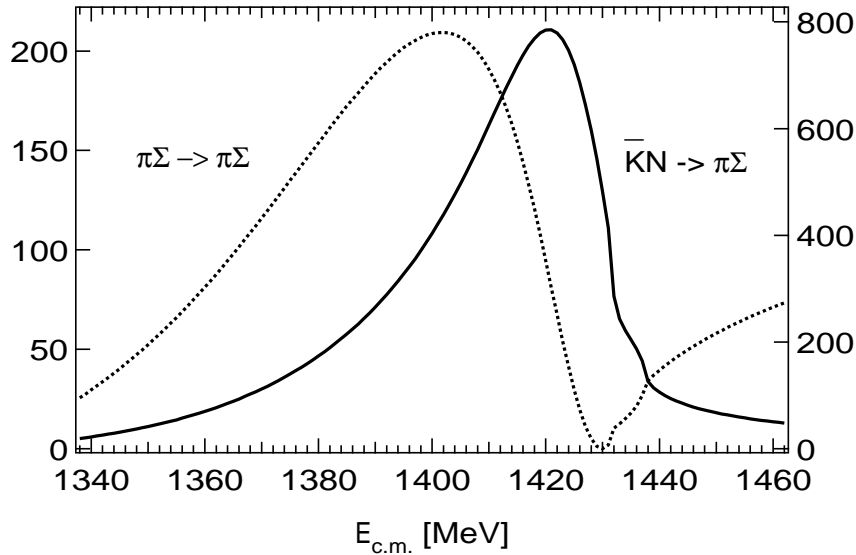
Figure 2. The $\pi\Sigma$ mass distributions with $I = 0$ constructed from the $\bar{K}N \to \pi\Sigma$ and $\pi\Sigma \to \pi\Sigma$ amplitudes. The solid and dashed lines denote $|T_{\bar{K}N\to\pi\Sigma}|^2 q_\pi$ and $|T_{\pi\Sigma\to\pi\Sigma}|^2 q_\pi$, respectively. Units are arbitrary.

5. Conclusions

In this talk we have shown the poles appearing in the meson–baryon scattering matrix for strangeness $S = -1$ within a coupled–channel chiral unitary approach, using two different methods for breaking the SU(3) symmetry which have been used in the literature.

In both approaches a set of resonances is generated dynamically from the interaction of the octet of pseudoscalar mesons with the octet of the $1/2^+$ baryons. The underlying SU(3) structure of the Lagrangians implies that, from the combination of the two original octets, a singlet and two octets of dynamically generated resonances should appear, but the dynamics of the problem makes the two octets degenerate in the case of exact SU(3) symmetry. The same chiral Lagrangians have mechanisms for chiral symmetry breaking which have as a consequence that the degeneracy is broken and two distinct octets appear. The breaking of the octet degeneracy has as a consequence that, in the physical limit, one of the $I = 0$ octet poles appears quite close to the singlet pole, and both of them are very close to the nominal $\Lambda(1405)$. These two resonances are quite close but different, the one at lower energies with a larger width and a stronger coupling to the $\pi\Sigma$ states than the one at higher energies, which couples mostly to the $\bar{K}N$ states. Thus we conclude that there is not just one single $\Lambda(1405)$ resonance, but *two*, and that what one sees in experiments is a *superposition* of these two states.

Another interesting finding is the suggestion that it is possible to find out the existence of the two resonances by performing different experiments, since in different experiments the weights by which the two resonances are excited are different. In this respect we call the attention to one reaction, $K^-p \to \Lambda(1405)\gamma$, which gives much weight to the

resonance which couples strongly to the $\bar{K}N$ states and, hence, leads to a peak structure in the invariant mass distributions which is narrower and appears at higher energies than the experimental $\Lambda(1405)$ peaks observed in hadronic experiments performed so far.

Finally, the findings discussed here about a possible $I = 1$ state close to the $\bar{K}N$ threshold and the experiment done in [20], which shows very distinct $\pi^+\Sigma^-$ and $\pi^-\Sigma^+$ distributions, deserve further attention and should lead in the near future to a clarification on the situation of this hypothetical state.

Acknowledgments

REFERENCES

1. M. Jones, R. H. Dalitz and R. R. Horgan, Nucl. Phys. B **129** (1977) 45.
2. N. Kaiser, T. Waas and W. Weise, Nucl. Phys. A **612** (1997) 297.
3. E. Oset and A. Ramos, Nucl. Phys. A **635** (1998) 99.
4. J. A. Oller and U.-G. Meißner, Phys. Lett. B **500** (2001) 263.
5. U.-G. Meißner, J. A. Oller, Phys. Rev. D **64** (2001) 014006.
6. P. J. Fink, G. He, R. H. Landau and J. W. Schnick, Phys. Rev. C **41** (1990) 2720.
7. D. Jido, A. Hosaka, J. C. Nacher, E. Oset and A. Ramos, Phys. Rev. C **66** (2002) 025203.
8. C. Garcia-Recio, J. Nieves, E. Ruiz Arriola and M. J. Vicente Vacas, arXiv:hep-ph/0210311.
9. G. Ecker, Prog. Part. Nucl. Phys. **35** (1995) 1; V. Bernard, N. Kaiser and U.-G. Meißner, Int. J. Mod. Phys. E **4** (1995) 193; A. Pich, Rept. Prog. Phys. **58** (1995) 563; U.-G. Meißner, Rept. Prog. Phys. **56** (1993) 903.
10. E. Oset, A. Ramos and C. Bennhold, Phys. Lett. B **527** (2002) 99 [Erratum-ibid. B **530** (2002) 260].
11. A. Ramos, E. Oset and C. Bennhold, Phys. Rev. Lett. **89** (2002) 252001.
12. N. Kaiser, P. B. Siegel and W. Weise, Nucl. Phys. A **594** (1995) 325.
13. T. Inoue, E. Oset and M. J. Vicente Vacas, Phys. Rev. C **65** (2002) 035204.
14. J. A. Oller and E. Oset, Nucl. Phys. A **620** (1997) 438 [Erratum-ibid. A **652** (1999) 407].
15. J. A. Oller, E. Oset and J. R. Peláez, Phys. Rev. D **59** (1999) 074001 [Erratum-ibid. D **60** (1999) 099906].
16. J. A. Oller and E. Oset, Phys. Rev. D **60** (1999) 074023.
17. N. Kaiser, Eur. Phys. J. A **3** (1998) 307.
18. D. Jido, J. A. Oller, E. Oset, A. Ramos and U. G. Meissner, Nucl. Phys. A **725** (2003) 181.
19. J. C. Nacher, E. Oset, H. Toki and A. Ramos, Phys. Lett. B **455**, 55 (1999).

20. J. K. Ahn et al., Proceedigns of the XVI Particles and Nuclei International Conference (PANIC02), Eds. K. Imai, T. Kishimodo and H. Toki, Nucl. Phys. A, in print.
21. T. Hyodo, A. Hosaka, E. Oset, A. Ramos and M. J. Vicente Vacas, arXiv:nucl-th/0307005.
22. J. C. Nacher, E. Oset, H. Toki and A. Ramos, Phys. Lett. B **461** (1999) 299.